

A NOVEL DTC SCHEME FOR A FIVE-LEVEL VOLTAGE SOURCE INVERTER WITH GTO THYRISTORS

R. Zaimeddine

Department of Electrical Engineering
University of Mouloud Mammeri, Algeria

E.M. Berkouk

laboratoire commande des processus
Ecole National Polytechnique, El Harache

Abstract - The object of this paper is to study a new control structure for sensorless induction machine dedicated to electrical drives using a five-level voltage source inverter (VSI). The output voltages of the three-level VSI can be represented by four groups : the zero voltage vectors, the small voltage vectors, the middle voltage vectors and the large voltage vectors in (d , q) plane. Then, the amplitude and the rotating velocity of the flux vector can be controlled freely. Both fast torque and optimal switching logic can be obtained. The selection is based on the value of the stator flux and the torque. This paper investigates a new control structure using a five-level voltage source inverter. Compared to classical Field Oriented Control (FOC), which necessitates generally three feedback loops with PI regulators, a current-regulated PWM converter, and two coordinate transformations, Direct Torque Control (DTC) uses only a couple of hysteresis comparators to perform both torque and flux dynamic control.

Both approaches are simulated for a induction motor. The results obtained with a novel DTC structure show superior performances over the FOC one without need to any mechanical sensor.

Key Words : Direct Torque Control, Flux Estimators, induction motor, optimisation criterion, multi-level inverter

1 Introduction

The rapid development of the capacity and switching frequency of the power semiconductor devices and the continuous advance of the power electronics technology have made many changes in static power converter systems and industrial motor drive areas. The conventional GTO inverters have limitation of their dc-link voltage. Hence, the series connections of the existing GTO thyristors have been essential in realizing high voltage and large capacity inverter configurations with the dc-link voltage [1]. The vector control of induction motor drive has made it possible to be used in applications requiring fast torque control such as traction [2]. In a perfect field oriented control, the decoupling characteristics of the flux and torque are affected highly by the parameter variation in the machine.

This paper describes a control scheme for direct torque and flux control of induction machines fed by a five-level inverter using a switching table. In this method, the output voltage is selected and applied sequentially to the machine through a look-up table so that the flux is kept constant and the torque is controlled by the rotating speed of the stator flux. The direct torque control (DTC) is one of the actively researched control scheme which is based on the decoupled control of flux and torque

providing a very quick and robust response with a simple control construction in ac drives [3], [4].

2 Three-Level Inverter Topology and The NPC Voltage Source

Fig. 1 shows the schematic diagram of neutral point clamped (NPC) three-level VSI. Each phase of this inverter consists of two clamping diodes, four GTO thyristors and four freewheeling diodes. Table.1 shows the switching states of this inverter.

Since three kinds of switching states exist in each phase, a three level inverter has 27 switching states.

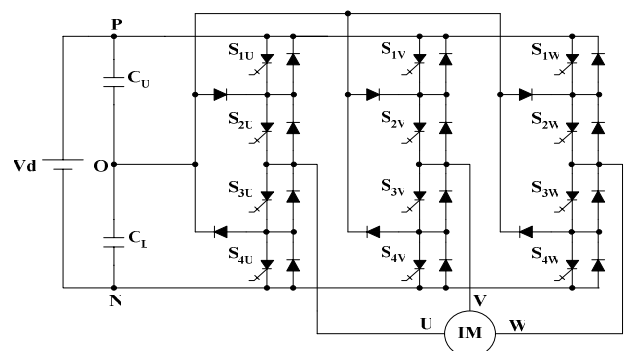


Fig. 1 : Schematic diagram of a three-level GTO inverter

Switching states	S ₁	S ₂	S ₃	S ₄	V _N
P	ON	ON	OFF	OFF	V _d
O	OFF	ON	ON	OFF	V _d /2
N	OFF	OFF	ON	ON	0

Table. 1: Switching states of a three-level inverter

A two-level inverter is only capable to produce six non-zero voltage vectors and two zero vectors [2]. Fig.2 shows the representation of the space voltage vectors of a three-level inverter for all switching states. According to the magnitude of the voltage vectors, we divide them into four groups : the zero voltage vectors (V₀), the small voltage vectors (V₁, V₄, V₇, V₁₀, V₁₃, V₁₆), the middle voltage vectors (V₃, V₆, V₉, V₁₂, V₁₅, V₁₈), the large voltage vectors (V₂, V₅, V₈, V₁₁, V₁₄, V₁₇). The zero voltage vector (ZVV) has three switching states, the small voltage vector (SVV) have two, and both the middle voltage vector (MVV) and the large voltage vector (LVV) have only one [1].

3 Induction Machine

Torque control of an asynchronous motor can be achieved on the basis of its model developed in a two axes (d , q) reference frame stationary with the stator winding. In this reference frame and with conventional notations, the electrical mode is described by the following equations:

$$\frac{di_{sd}}{dt} = -\frac{1}{\sigma T_r L_s} \varphi_{sd} + \frac{p\Omega}{\sigma L_s} \varphi_{sq} - \frac{1}{\sigma} \left(\frac{1}{T_r} + \frac{1}{T_s} \right) i_{sd} - p\Omega i_{sq} + \frac{1}{\sigma L_s} V_{sd} \quad (1)$$

$$\frac{di_{sq}}{dt} = -\frac{p\Omega}{\sigma L_s} \varphi_{sd} + \frac{1}{\sigma T_r L_s} \varphi_{sq} - \frac{1}{\sigma} \left(\frac{1}{T_r} + \frac{1}{T_s} \right) i_{sq} + p\Omega i_{sd} + \frac{1}{\sigma L_s} V_{sq} \quad (2)$$

$$\frac{d\varphi_{sd}}{dt} = V_{sd} - R_s i_{sd} \quad (3)$$

$$\frac{d\varphi_{sq}}{dt} = V_{sq} - R_s i_{sq} \quad (4)$$

The mechanical mode associated to the rotor motion is described by :

$$J \frac{d\Omega}{dt} = \Gamma_{em} - \Gamma_r(\Omega) \quad (5)$$

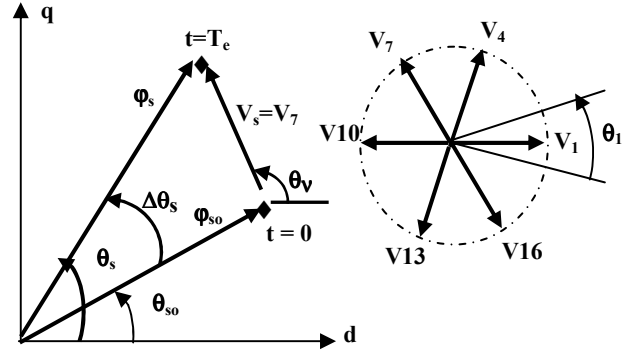
$\Gamma_r(\Omega)$ and Γ_{em} are respectively the load torque and the electromagnetic torque developed by the machine.

4 Stator Flux and Torque Estimation

Basically, DTC schemes require the estimation of the stator flux and torque. The stator flux evaluation can be carried out by different techniques depending on whether the rotor angular speed or (position) is measured or not. For sensorless application, the “voltage model” is usually employed. The stator flux can be evaluated by integrating from the stator voltage equation.

$$\varphi_s(t) = \int (V_s - R_s I_s) dt \quad (6)$$

This method is very simple requiring the knowledge of the stator resistance only. The effect of an error in R_s is usually quite negligible at high excitation frequency but becomes more serious as the frequency approaches zero [5].



Different switching strategies can be employed to control the torque according to whether the flux has to be reduced or increased.

Each strategy affect the drive behavior in terms of torque and current ripple, switching frequency and two or four-quadrant operation capability. Assuming the voltage drop $R_s i_s$ small, the head of the stator flux ϕ_s moves in the direction of stator voltage V_s at a speed proportional to the magnitude of V_s according to

$$\Delta\phi_s = V_s T_e \quad (9)$$

The switching configuration is made step by step, in order to maintain the stator flux and torque within limits of two hysteresis bands. Where T_e is the period in which the voltage vector is applied to stator winding. Selecting step by step the voltage vector appropriately, it is then possible to drive ϕ_s along a prefixed track curve.

Assuming the stator flux vector lying in the k -th sector ($k=1,2,3,4,5,6$) of the (d, q) plane, in the case of three-level inverter, to improve the dynamic performance of DTC at low speed and to allow four-quadrant operation, it is necessary to involve the voltage vectors V_{K-1} and V_{K-2} in torque and flux control. In the following, V_{K-1} and V_{K-2} will be denoted "backward" voltage vectors in contraposition to "forward" voltage vectors utilised to denote V_{K+1} and V_{K+2} . A simple strategy which makes use of these voltage vectors is shown in table.2. The conventional DTC has been studied.

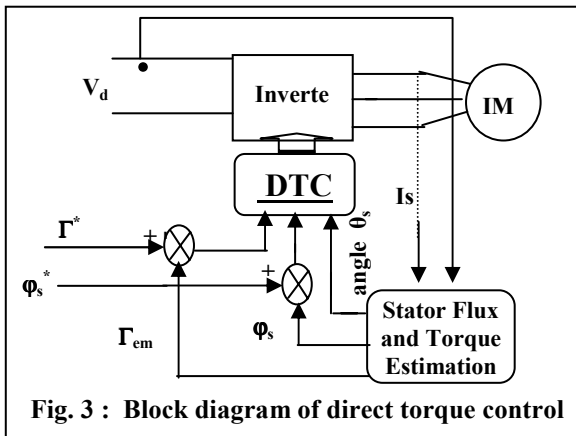


Fig. 3 : Block diagram of direct torque control

	$\Gamma_{em} \uparrow$	$\Gamma_{em} \downarrow$
$\phi_s \uparrow$	V_{K+1}	V_{K-1}
$\phi_s \downarrow$	V_{K+2}	V_{K-2}

Table.2 : Selection strategy for four-quadrant operation

According to this strategy, the stator flux vector is required to rotate in both positive and negative directions. By this, even at very low shaft speed, large negative values of rotor angular frequency can be achieved, which are required when the torque is to be decreased very fast. Furthermore, the selection strategy represented in table.2 allows good flux control to be obtained even in the low speed range. However, the high dynamic performance which can be obtained utilising voltage vectors having large components tangential to the stator vector locus implies very high switching frequency.

6 Five Level Inverter Topology and the NPC Voltage Source

Fig. 4 shows the schematic diagram of neutral point clamped (NPC) five-level VSI. Each phase of this inverter consists of two clamping diodes, six GTO thyristors and six freewheeling diodes in series, of two other in parallel. Table.3 shows the switching states of this inverter.

Since five kinds of switching states exist in each phase, a five level inverter has 125 switching states.

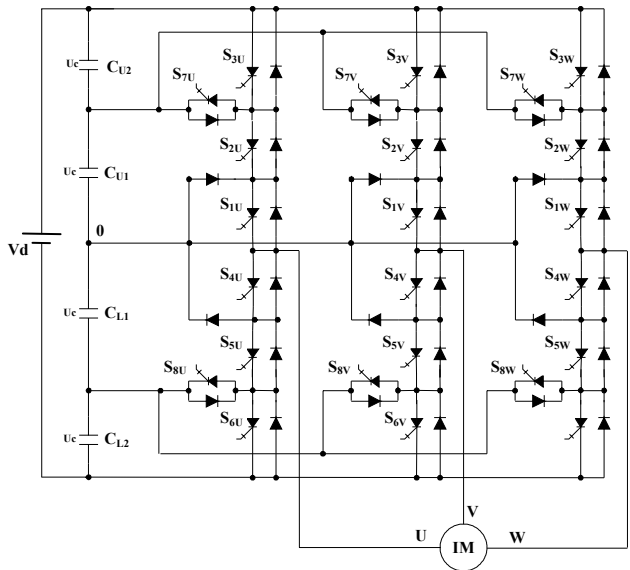


Fig. 4 : Schematic diagram of a five-level GTO inverter

Switching states	S_{1x}	S_{2x}	S_{3x}	S_{4x}	S_{5x}	S_{6x}	V_x
L1	OFF	OFF	OFF	ON	ON	ON	$-2U_c$
L2	OFF	OFF	ON	ON	ON	OFF	$-U_c$
L3	OFF	ON	OFF	OFF	ON	ON	0
L4	ON	OFF	ON	ON	OFF	OFF	0
L5	ON	ON	OFF	OFF	OFF	ON	U_c
L6	ON	ON	ON	OFF	OFF	OFF	$2U_c$

Table. 3 : Switching states of a Five-level inverter ($x = U, V, W$)

Fig.5 shows the representation of the space voltage vectors of a five-level inverter for all switching states. According to the magnitude of the voltage vectors, we divide them into nine groups :

(V_0) ; $(V_1, V_{11}, V_{21}, V_{31}, V_{41}, V_{51})$; $(V_7, V_{17}, V_{27}, V_{37}, V_{47}, V_{57})$; $(V_2, V_{12}, V_{22}, V_{32}, V_{42}, V_{52})$; $(V_6, V_9, V_{16}, V_{19}, V_{26}, V_{29}, V_{36}, V_{39}, V_{46}, V_{49}, V_{56}, V_{59})$; $(V_3, V_{13}, V_{23}, V_{33}, V_{43}, V_{53})$; $(V_8, V_{18}, V_{28}, V_{38}, V_{48}, V_{58})$; $(V_5, V_{10}, V_{15}, V_{20}, V_{25}, V_{30}, V_{35}, V_{40}, V_{45}, V_{50}, V_{55}, V_{60})$; $(V_4, V_{14}, V_{24}, V_{34}, V_{44}, V_{54})$.

The zero voltage vector (ZVV) has five switching states, the large voltage vector (LVV) have only one.

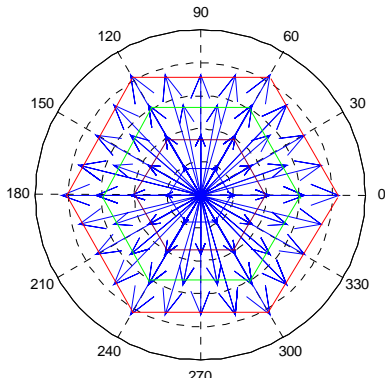


Fig.5 : Space voltage vectors of a five-level inverter

7 Direct Torque Control Using A Five-Level Inverter

A switching table is used to select the best output voltage depending on the position of the stator flux and desired action on the torque and stator flux. The flux position in the (d, q) plane is quantified in six sectors. Alternative tables exist for specific operation mode. The switching table for the case of a two-level or a three-level inverter, it is easily possible to expand the optimal vector selection to include the larger number of voltage vectors produced by five-level inverter. The appropriate vector voltage is selected in the order to reduce the number of commutation and the level of steady-state ripple.

For flux control, let the variable E_ϕ ($E_\phi = \phi_s^* - \phi_s$) be located in one of the three regions fixed by the constraints:

$$E_\phi < E_{\phi \min}, E_{\phi \min} \leq E_\phi \leq E_{\phi \max}, E_\phi > E_{\phi \max}.$$

The switable flux level is then bounded by $E_{\phi \min}$ and $E_{\phi \max}$. The flux control is made by two-level hysteresis comparator. Three regions for flux location are noted, flux as in fuzzy control schemes, by $E_{\phi n}$ (negative), $E_{\phi z}$ (zero) and $E_{\phi p}$ (positive).

A high level performance torque control is required. To improve the torque control let of the mismatch E_Γ ($E_\Gamma = \Gamma_{em}^* - \Gamma_e$) to belong to one of the seven regions defined by the constraints :

$$E_\Gamma < E_{\Gamma \min 3}, E_{\Gamma \min 3} \leq E_\Gamma \leq E_{\Gamma \min 2}, E_{\Gamma \min 2} \leq E_\Gamma \leq E_{\Gamma \min 1}, E_{\Gamma \min 1} \leq E_\Gamma \leq E_{\Gamma \max 1}, E_{\Gamma \max 1} \leq E_\Gamma \leq E_{\Gamma \max 2}, E_{\Gamma \max 2} \leq E_\Gamma \leq E_{\Gamma \max 3} \text{ and } E_{\Gamma \max 3} < E_\Gamma.$$

The seven regions defined for torque location are also noted, as in fuzzy control schemes, by $E_{\Gamma nl}$ (negative large), $E_{\Gamma nm}$ (negative medium), $E_{\Gamma ns}$ (negative small), $E_{\Gamma z}$ (zero), $E_{\Gamma ps}$ (positive small), $E_{\Gamma pm}$ (positive medium) and $E_{\Gamma pl}$ (positive large). The torque is then controlled by an hysteresis comparator built with three lower bounds and three upper known bounds.

8 Switching Strategy

The switching strategy in the order of the sector θ_s , is illustrate by each tables. The flux and torque control by vector voltage has in nature a desecrate behavior. In fact, we can easily verify that the same vector could be adequate for a set of value of θ_s . the number of sectors should be as large as possible to have an adequate decision.

For this reason, we propose a new approach for direct torque control using a three-level inverter based on twelve regular sectors noted by θ_1 to θ_{12} .

θ_1				θ_2				θ_3			
$E_\Gamma \backslash E_\phi$	P	Z	N	$E_\Gamma \backslash E_\phi$	P	Z	N	$E_\Gamma \backslash E_\phi$	P	Z	N
PL1	14	17	24	PL1	14	17	24	PL1	24	27	34
PL2	15	17	25	PL2	20	17	30	PL2	25	27	35
PM1	18	17	28	PM1	18	17	28	PM1	28	27	38
PM2	13	11	23	PM2	13	11	23	PM2	23	21	33
PS1	9	11	19	PS1	16	11	26	PS1	19	21	29
PS2	12	11	22	PS2	12	11	22	PS2	22	21	32
Z	0	0	0	Z	0	0	0	Z	0	0	0
NS2	52	0	42	NS2	52	0	42	NS2	2	0	52
NS1	56	41	46	NS1	59	41	49	NS1	6	51	56
NM2	53	47	43	NM2	53	47	43	NM2	3	57	53
NM1	58	42	48	NM1	58	42	48	NM1	8	52	58
NL2	55	46	45	NL2	55	49	50	NL2	5	59	55
NL1	54	43	44	NL1	54	43	44	NL1	4	53	54

θ4				θ5				θ6			
E _φ \ E _r	P	Z	N	E _φ \ E _r	P	Z	N	E _φ \ E _r	P	Z	N
PL1	24	27	34	PL1	34	37	44	PL1	34	37	44
PL2	30	27	40	PL2	35	37	45	PL2	40	37	50
PM1	28	27	38	PM1	38	37	48	PM1	38	37	48
PM2	23	21	33	PM2	33	31	43	PM2	33	31	43
PS1	26	21	36	PS1	29	31	39	PS1	36	31	46
PS2	22	21	32	PS2	32	31	42	PS2	32	31	42
Z	0	0	0	Z	0	0	0	Z	0	0	0
NS2	2	0	52	NS2	12	0	2	NS2	12	0	2
NS1	9	51	9	NS1	16	1	6	NS1	19	1	9
NM2	3	57	53	NM2	13	7	3	NM2	13	7	3
NM1	8	52	58	NM1	18	2	8	NM1	18	2	8
NL2	10	59	55	NL2	15	6	5	NL2	20	9	10
NL1	4	53	54	NL1	14	3	4	NL1	14	3	4

θ7				θ8				θ9			
E _φ \ E _r	P	Z	N	E _φ \ E _r	P	Z	N	E _φ \ E _r	P	Z	N
PL1	44	47	54	PL1	44	47	54	PL1	54	57	4
PL2	45	47	55	PL2	50	47	60	PL2	55	57	5
PM1	48	47	58	PM1	48	47	58	PM1	58	57	8
PM2	43	41	53	PM2	43	41	53	PM2	53	51	3
PS1	39	41	49	PS1	46	41	56	PS1	49	51	9
PS2	42	41	52	PS2	42	41	52	PS2	52	51	2
Z	0	0	0	Z	0	0	0	Z	0	0	0
NS2	22	0	12	NS2	22	0	12	NS2	32	0	22
NS1	26	11	16	NS1	29	11	19	NS1	36	21	26
NM2	23	17	13	NM2	23	17	13	NM2	33	27	23
NM1	28	12	18	NM1	28	12	18	NM1	38	22	28
NL2	25	16	15	NL2	30	19	20	NL2	35	26	25
NL1	24	13	14	NL1	24	13	14	NL1	34	23	24

θ10				θ11				θ12			
E _φ \ E _r	P	Z	N	E _φ \ E _r	P	Z	N	E _φ \ E _r	P	Z	N
PL1	54	57	4	PL1	4	7	14	PL1	4	7	14
PL2	55	57	10	PL2	5	7	15	PL2	10	7	20
PM1	58	57	8	PM1	8	7	18	PM1	8	7	18
PM2	53	51	3	PM2	3	1	13	PM2	3	1	13
PS1	56	51	6	PS1	59	1	9	PS1	6	1	16
PS2	52	51	2	PS2	2	1	12	PS2	2	1	12
Z	0	0	0	Z	0	0	0	Z	0	0	0
NS2	32	0	22	NS2	42	0	32	NS2	42	0	32
NS1	39	21	29	NS1	46	31	36	NS1	49	31	39
NM2	33	27	23	NM2	43	37	33	NM2	43	37	33
NM1	38	22	28	NM1	48	32	38	NM1	48	32	38
NL2	40	29	30	NL2	47	36	35	NL2	50	39	40
NL1	34	23	24	NL1	44	33	34	NL1	44	33	34

8 The Simulation Results

The validity of the proposed DTC algorithm for five-level voltage source inverter is proved by the simulation results using Matlab-Simulink. The parameters of motors are given in the Appendix. The used flux and torque emismathes for the

approach are expressed in percent with respect to th flux and torque reference values.

$E_{\phi \max} = 3\%$, $E_{\phi \min} = -3\%$. $E_{\Gamma \min 1} = -3\%$, $E_{\Gamma \min 2} = -2.8\%$, $E_{\Gamma \min 3} = -2.6\%$, $E_{\Gamma \min 4} = -2.25\%$, $E_{\Gamma \min 5} = -1.5\%$, $E_{\Gamma \min 6} = -0.95\%$, $E_{\Gamma \max 1} = 0.95\%$, $E_{\Gamma \max 2} = 1.5\%$, $E_{\Gamma \max 3} = 2.25\%$, $E_{\Gamma \max 4} = 2.6\%$, $E_{\Gamma \max 5} = 2.8\%$, $E_{\Gamma \max 6} = 3\%$.

In the case of a three level-inverter :

$E_{\phi \max} = 3\%$, $E_{\phi \min} = -3\%$. $E_{\Gamma \min 1} = -0.8\%$, $E_{\Gamma \min 2} = -3\%$, $E_{\Gamma \max 1} = 0.8\%$, $E_{\Gamma \max 2} = 3\%$.

However, the machine has been supposed to run at load.

$$\Gamma_r = \left(\frac{\Gamma_{em}}{\Omega_{ref}} - K_f \right) \cdot \Omega \quad (10)$$

The simulation results illustrates both the steady state and the transient performance of the proposed torque control scheme. The wave form of the stator current is closed to a sinusoidal signal. The trajectory of the flux in the case of the new approach, (five level control), is nearly a circle compared to the flux response in the conventional DTC, (three level control), and fast torque is obtained.

Fig.6 shows the phase current and flux for steady state operation and transient régime at 9 N.m with 0.9 Wb. The wave form of the stator current is closed to a sinusoidal signal, The phase current generated by the five-level inverter have low harmonic components and low torque ripple is observed in the fig.7.

The trajectory of the flux in the case of the new approach is nearly a circle and answers more quickly compared to the flux response in the conventional DTC. Fig.8 shows the torque reverse response from + 9 N.m to - 9 N.m and flux for 0.9 Wb. The output torque reaches the new reference torque in about 8 ms, fast torque response is obtained.

From this analysis high dynamic performance, good stability and precision are achieved.

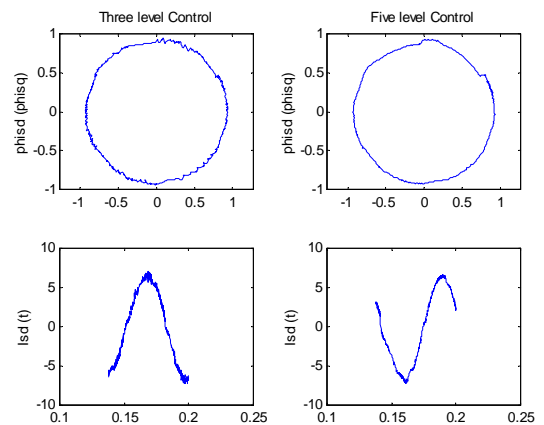


Fig. 6 : Vector flux locus and current response

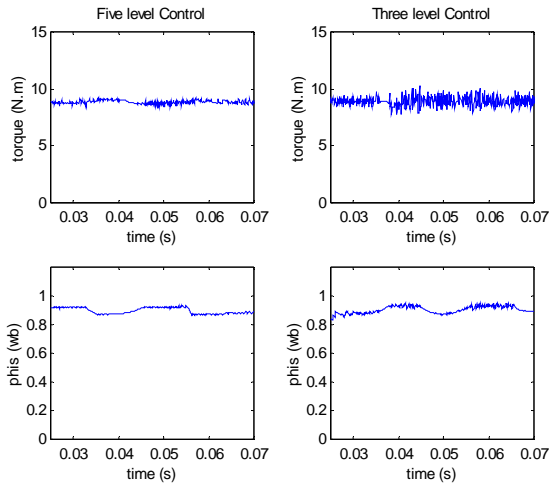


Fig. 7 : Torque response and flux

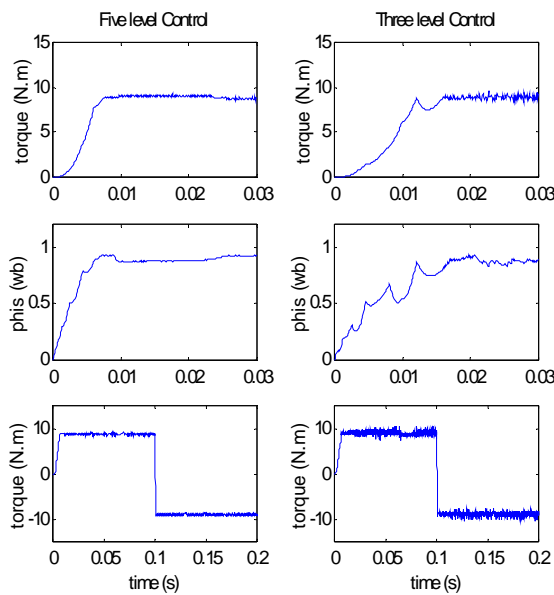


Fig. 8 : Torque and flux response

10 Conclusion

The direct torque control DTC was introduced to give a fast and good dynamic torque and can be considered as an alternative to the field oriented control FOC technique. Two problems usually associated with DTC drives which are based on hysteresis comparators are: variable switching frequency and inaccurate stator flux estimation which can degrade the drive performance. The effect of proposed method has been proven by simulations. It is concluded that the proposed control produces better results for transient state operation and steady state then the conventional control.

In this paper, a DTC systems using five-level GTO voltage source inverter is presented it is suitable for high-power and high-voltage applications. We enhance the DTC approach by introducing two

multi-level hysteresis comparators for flux and torque control.

Appendix

List of the used notations

d, q : indices for (d, q) components ; s, r : indices variables ; L : magnetizing Inductance ; L_m : mutual inductance ; V : voltage ; i : current ; ϕ : flux ; R : resistance ; Γ_{em} : electromagnetic torque ; J : rotor inertia ; P : number of pairs of poles ; ω_s : statoric pulsation ; V_d : dc-link voltage ; K_f : friction Coefficient ; T_e : sampling time ; E : error of the variables ; ω_r : electric rotor speed ; $\Omega = p \omega_r$; σ : leakage coefficient ; T_r : rotor time response ; T_s : stator time response.

Induction Motors Parameters

Rated power : 1.5 kW ; Rated voltage : 220 V ; Rated speed : 1420 rpm ; Rated frequency : 50 Hz ; Rated current : 3.64 A (Y) et 6.31 (Δ) ; Stator resistance : 4.85 Ω ; Rotor resistance : 3.805 Ω ; Stator inductance : 0.274 H ; Rotor inductance : 0.274 H ; Magnetizing Inductance : 0.258 H ; Number of poles : 2 ; Rotor inertia : 0.031 Kg.m² ; Friction Coefficient : 0.008 N.m.s/rd ; $V_{dc} = 514$ v ; $T_e = 100$ μ s.

References

- [1] Y.H. Lee, B.S. Suh, and D.S. Hyan, "A novel PWM scheme for a three-level voltage source inverter with GTO thyristors". *IEEE Trans. on Ind. Appl.*, vol. 33 2, March\April 1996, pp. 260-268.
- [2] I. Takahashi and T. Noguchi, "A new quick-response and high-efficiency control strategy of an induction motor". *IEEE Trans. on IA*, vol. 22, No. 5, Sept\Octo 1986, pp. 820-827.
- [3] J.C. Trounce, S.D. Round, and R.M. Duke, "Comparison by simulation of three-level induction motor torque control schemes for electrical vehicle applications". *Proc. of international power engineering conference*, vol. 1, May 2001, pp. 294-299.
- [4] WU. Xuezh, and L. Huang, "Direct torque control of three-level inverter using neural networks as switching vector selector". *IEEE IAS, annual meeting*, 30 September\ 04 October 2001.
- [5] D. Casadei, G. Grandi, G. Serra, and A. Tani, "Switching strategies in direct torque control of induction machines". *ICEM 94*, vol. 2, 1994, pp. 204-209.